

nuQmm: Quantized MatMul for Efficient Inference of Large-Scale Generative Language Models

Gunho Park^{*†}, Baeseong Park^{*‡}, Se Jung Kwon[‡], Byeongwook Kim[‡], Youngjoo Lee[†], and Dongsoo Lee[‡]

[†]Pohang University of Science and Technology, Pohang, Republic of Korea

{gunho1123, youngjoo.lee}@postech.ac.kr

[‡]NAVER CLOVA, Seongnam, Republic of Korea

{baeseong.park, sejung.kwon, byeonguk.kim, dongsoo.lee}@navercorp.com

Abstract—The recent advance of self-supervised learning associated with the Transformer architecture enables natural language processing (NLP) to exhibit extremely low perplexity. Such powerful models demand ever-increasing model size, and thus, large amounts of computations and memory footprints. In this paper, we propose an efficient inference framework for large-scale generative language models. As the key to reducing model size, we quantize weights by a non-uniform quantization method. Then, quantized matrix multiplications are accelerated by our proposed kernel, called nuQmm, which allows a wide trade-off between compression ratio and accuracy. Our proposed nuQmm reduces the latency of not only each GPU but also the entire inference of large LMs because a high compression ratio (by low-bit quantization) mitigates the minimum required number of GPUs. We demonstrate that nuQmm can accelerate the inference speed of the GPT-3 (175B) model by about 14.4 times and save energy consumption by 93%.

Index Terms—Non-Uniform Quantization, Model Compression, Generative Language Model, Deep Learning, Transformer, AI Inference

I. INTRODUCTION

Recent years have observed large-scale language models presenting state-of-the-art performance on various natural language process (NLP) tasks. Such rapid progress in NLP performance has been highly facilitated by the self-supervised learning method. Through self-supervised learning, a model is first pre-trained by using unlabeled data and then fine-tuned by a small number of labeled data [1]–[4]. Since pre-training dominates the entire training process without an expensive labeling process, the size of the training dataset can substantially increase. Combined with efficient sequence-to-sequence model architectures, such as the Transformers [5], the number of model parameters also significantly increases.

As for NLP tasks, it is reported that LM performance follows predictable power-law scaling as a function of model size [6], [7]. Since then, especially for generative LMs, researchers proposed numerous large-scale models including GPT-3 (175B) [6], HyperCLOVA (204B) [8], Gopher (280B) [9], and Megatron Turing NLG (530B) [10]. Note that models of billions of parameters cannot be accommodated by one GPU since GPU memory size is sacrificed and limited in order to enhance memory bandwidth [11], [12]. To address such concerns, model parallelism has been suggested to distribute computations over multiple GPUs through GPU-to-GPU communication [13], [14]. As shown in Fig. 1, model parallelism

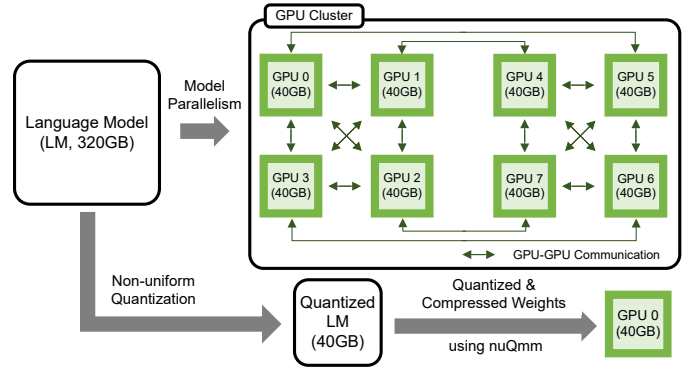


Fig. 1. A large language model deployed with 8 GPUs supported by model parallelism, or with 1 GPU only using quantized weights. Assuming 40GB GPU memory size, 8 GPUs are required to serve a 320GB language model unless model compression is engaged.

splits parameters of a large LM model into numerous GPUs, and information during training/inference can be shared among GPUs through dedicated channels.

Model parallelism can be divided into tensor parallelism and pipeline parallelism to improve latency and throughput, respectively. Such parallelism schemes, however, require various communication primitives, such as AllReduce, Reduce, Broadcast, and AllGather, to synchronize partial outputs produced by GPUs [15]. Even though GPU-specific external communication protocols (e.g., NVLink [16]) can reduce communication latency, an inherent variance of GPU performance (caused by various random factors such as fabrication process variation and operating system conditions) is another performance bottleneck [17]. In addition, since a large matrix is separated into submatrices, each GPU faces tall-and-skinny matrix multiplications with low utilization of resources [18], [19]. As a result, performance gain by model parallelism becomes a sub-linear function of the number of GPUs.

To alleviate the challenges of model parallelism, parameter quantization [20]–[22] is a practical solution to reduce the model size such that the number of GPUs to serve inference can be lower, as described in Fig. 1. Among various quantization schemes, uniform quantization is a popular choice since we can exploit integer-based arithmetic units [23]–[26]. Uniform quantization, however, is practically limited to 8 bits

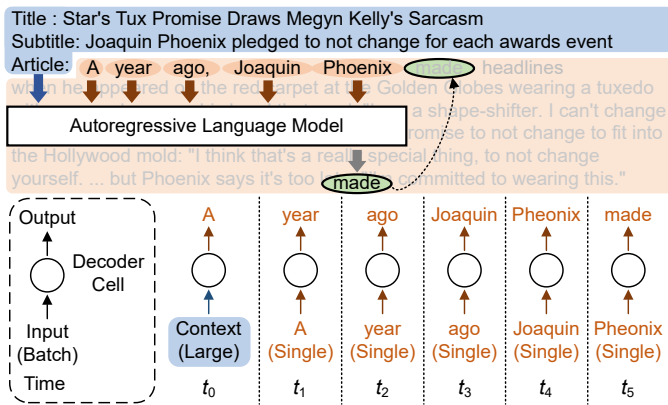


Fig. 2. An illustration of the autoregressive language model. Given an input context, a single token is generated for each iteration. The entire generation procedure can be categorized into the summarization stage (along with a large batch size using an input context) and the generation stage executing single-batch operations using the previously generated token.

while non-linear operations (e.g., softmax and normalization techniques) can be imprecise [27], [28]. Moreover, activation quantization/dequantization should be implemented on-the-fly on top of the requirement of accurate estimation of the distribution of activations in advance.

In this paper, we consider non-uniform quantization to achieve a high compression ratio. Specifically, we utilize binary-coding quantization (BCQ) scheme [29] to gain benefits of simple arithmetic operations. Note that non-uniform quantization inherently relies on customized hardware to support bit-level operations. To enable efficient BCQ scheme for inference on GPUs, we propose a new BCQ-dedicated matrix multiplication kernel, called nuQmm, to obtain low inference latency while avoiding the necessity of activation quantization. Our major contributions in this work include the following:

- Compared to the previously proposed matrix multiplication kernels with quantized parameters, nuQmm provides a wide search space of trade-offs between compression ratio and latency (based on GPU-specific efficient hardware utilization method to implement various BCQ formats).
- Under such new search space, we quantize a few well-known generative LMs, such as GPT-2 and GPT Neo, to investigate the range of compression ratio achievable by nuQmm.
- For large LMs, we show that nuQmm can considerably accelerate matrix multiplications with small quantization bits while power consumption is saved a lot by reducing the number of GPUs. Consequently, nuQmm leads to low energy consumption.
- In the case of GPT-3 (175B), our experimental results show that matrix multiplications can be accelerated by about 14.4 times while overall energy consumption can be saved by 93%.

TABLE I
SIZES, ARCHITECTURES, AND RELEASE TYPES OF VARIOUS GENERATIVE LANGUAGE MODELS

Model Name	n_{params}	n_{layers}	d_{model}	Release
GPT-2 Small	124M	12	768	Public
GPT-2 Medium	355M	24	1024	Public
GPT-2 Large	774M	36	1280	Public
GPT-2 XL	1.5B	48	1600	Public
GPT Neo 1.3B	1.3B	24	2048	Public
GPT Neo 2.7B	2.7B	32	2560	Public
GPT-J 6B	6.1B	28	4096	Public
GPT-3 6.7B	6.7B	32	4096	Private
GPT-3 13B	13.0B	40	5140	Private
GPT-3 175B	175.0B	96	12288	Private
MT-NLG	530.0B	105	20480	Private

II. BACKGROUND

A. Generative Language Models

Well-known large-scale generative LMs, such as GPT-3, are autoregressive models that predict future tokens using the previous tokens in a feed-forward fashion. For example, as shown in Fig. 2, assuming an input context is given (for in-context learning [6]), a new token can be predicted by using the previously generated tokens. Correspondingly, autoregressive modeling employs both large-batch operations (for the summarization stage conducting in-context learning using a given input context) and single-batch operations (for the generation stage to generate a single token at a time index).

Since the Transformer introduced a self-attention mechanism and a parallelized training algorithm for autoregressive models using a teacher forcing technique [5], virtually all large-scale generative LMs follow the decoder structure of the Transformer. In addition to the architectural advantages of the Transformer to scale the model size, generative LMs are increasing the number of parameters (as depicted in Table I) because: 1) self-supervised learning alleviates the burden of the expensive labeling process and 2) scaling-law [6], [7] provides a predictable performance on the cross-entropy loss as the model size increases. Surprising qualitative evaluation results (e.g., human-like writing) of extreme-scale LMs also fueled the competition in model size [8], [9].

B. GPU-Accelerated Generative LMs

For the Transformers and their variants, the processing time of matrix multiplications dominates the entire inference latency because of higher time complexity compared to activation functions, normalization layers, and so on [27], [28], [30]. To validate such a claim, Fig. 3 shows the latency breakdown of representative large-scale generative LMs (GPT-2 Medium, GPT Neo 1.3B, and GPT Neo 2.7B) with a various number of tokens to be generated. Fig. 3 is obtained by RTX-3090 and FasterTransformer inference framework of Nvidia¹. We can observe that matrix multiplications dominate the entire processing time (at least 80%) for various LM sizes and tokens to be generated. Hence, GPUs are widely adopted to accelerate inference because GPUs embed lots of arithmetic units and

¹<https://github.com/NVIDIA/FasterTransformer>

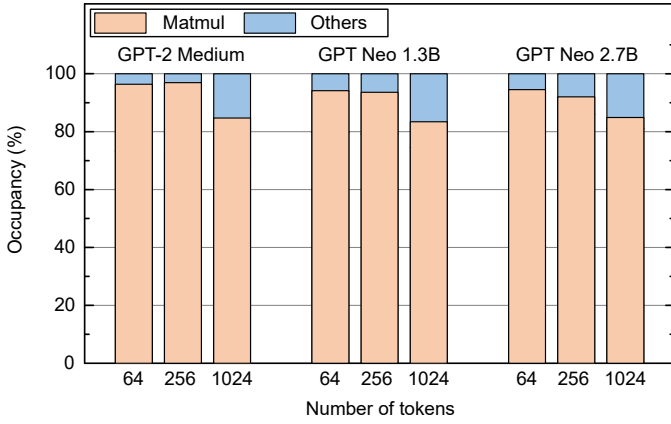


Fig. 3. Latency breakdown of GPT models with a different number of tokens to be generated. The overall performance is dominated by MatMul operations especially when a larger model size and a small number of tokens are employed. Experiments are conducted with RTX-3090 and FasterTransformer inference framework.

support multiple threads that are critical to expediting matrix multiplications [11], [14]. Note that extracting high performance from GPUs depends on arithmetic intensity. In other words, batch size should be large enough to ensure a high reuse ratio of data once retrieved from main memory [31]. In the extreme case of a single batch, matrix multiplication becomes memory-bound (in the form of a matrix-vector multiplication) such that utilization of internal arithmetic units is forced to be low. As such, for the generation stage (shown in Fig. 2) requiring single-batch operations, we can expect the speed of GPUs running generative LM inference to be far from peak performance. Another issue with running GPUs for inference is that GPUs have prioritized high memory bandwidth over memory size [31], [32]. Consequently, large LMs need to be distributed across multiple GPUs so as to incur GPU-to-GPU communication overhead.

C. Binary-Coding Quantization

Quantization reduces the number of bits to represent model parameters. Shrinking memory footprint by quantization for generative LMs is effective to address the concerns on GPU performance, namely, 1) memory-bound single-batch operations for generating tokens and 2) the usage of multiple GPUs and associated communication overhead. Note that various uniform quantization methods are being intensively studied because uniform quantization can be implemented by simple fixed-point operations [24], [27], [28], [33]. On the other hand, non-uniform quantization usually demands complicated operations of low parallelism while supporting hardware instructions may not be available [20], [34].

In this paper, we choose binary-coding quantization (BCQ), first introduced in [29], which is one of the non-uniform quantization schemes. When a weight vector \mathbf{w} (of size n) is quantized by BCQ and q is the number of quantization bits, \mathbf{w} is approximated to be $\sum_{i=1}^q \alpha_i \mathbf{b}_i$ where $\alpha_i \in \mathbb{R}^+$ is a scaling factor and $\mathbf{b}_i \in \{-1, +1\}^n$ is a binary vector. Note that a scaling factor α can be shared by many weights (n can be any

number) such that larger n value results in a relatively smaller memory footprint for scaling factors. The quantization process broadly involves finding scaling factors and binary vectors to minimize the quantization error as follows:

$$\arg \min_{\alpha, \mathbf{b}} \left\| \mathbf{w} - \sum_{i=1}^q \alpha_i \mathbf{b}_i \right\|^2, \quad (1)$$

which does not have analytical solutions except when $q = 1$. Thus, scaling factors and binary vectors are obtained by iterative search methods [20], [34] or by quantization-aware training [30]. In this work, we discuss the unique mathematical properties of BCQ to enable efficient quantized matrix multiplications.

III. DESIGN METHODOLOGY OF NUQMM

Our overall goal is to explore high-performance and low-energy inference systems for large-scale generative language models such as GPT-3 175B. To this end, an efficient quantization method is supposed to compress models with a high compression ratio while reducing quantization error (for given quantization bits) in consideration of the characteristics of large-scale LMs. In addition, a new kernel that efficiently supports such an efficient quantization technique is also necessary so that latency improvement through quantization can be maximized. In this section, we propose new advanced BCQ formats that can be supported by our proposed kernel nuQmm. The proposed nuQmm is designed to directly utilize binary weights in a compressed format without additional overhead such as dequantization. As a result, we demonstrate that we can reduce the number of GPUs to run large-scale LM inference.

A. Group-wise Binary-Coding Quantization

In practice, conventional BCQ methods assume that a scaling factor is assigned to each row of a weight matrix (or even to the entire matrix) so as to support vector instructions of CPUs or GPUs [20], [29]. As large-scale LMs introduce deeper and wider model structures along with ever-increasing parameter size [9], [13], however, we argue that such conventional row-wise BCQ format encounters various challenges. Suppose that a relatively small hidden size (e.g., $d_{\text{model}} = 1024$ in Table I) is selected along with small weight matrices correspondingly, row-wise assignment of scaling factors might be reasonable to obtain low quantization error. On the other hand, if the hidden size increases rapidly (e.g., $d_{\text{model}} = 12288$ for GPT-3 175B in Table I) according to the advent of large-scale LMs, it would be more difficult to compute a proper scaling factor shared by a larger number of weights. One possible solution to lower quantization error is to increase the number of quantization bits. Such a method, however, sacrifices the compression ratio considerably in a regime of low-bit quantization. As a result, for a given number of quantization bits, it is necessary to investigate different ways of assigning scaling factors as long as a new assignment can be backed by practical implementation.

Scale Factors	$m \times \frac{n}{g} \times q \times 32$ bits
Binary Weights	$m \times n \times q$ bit
Total Space	Scale Factors + Binary Weights

(a) Space complexity

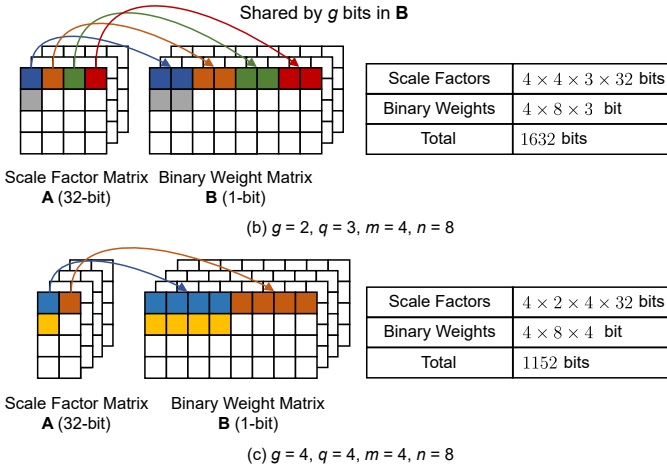


Fig. 4. Group-wise BCQ example with two different (g, q) configurations to quantize an (8×8) matrix. Assuming a scaling factor of 32 bits, smaller q can yield a larger memory footprint if g is also small.

a) *Group-wise α Assignment:* As an alternative to row-wise quantization, we propose group-wise quantization in which a scaling factor can be shared by an arbitrary number of weights. Our proposed new BCQ format introduces a new hyper-parameter g as a group size that represents the number of weights to be shared by a scaling factor. In this paper, g is a fixed number with a range of 8 (as the minimum) to the column width of a matrix (equivalent to row-wise quantization). Since g is a constant number, the hidden size does not affect our group-wise BCQ formats. We discuss how to implement the proposed group-wise BCQ efficiently on GPUs later.

b) *Impact on Compression Ratio:* For a given q (i.e., the number of quantization bits), a smaller group size g can lower quantization error at the expense of increased memory footprint for scaling factors. For a target quantization error, thus, a compression ratio is a compromise between q and g . In other words, due to the introduction of g , we can control the amount of scaling factors and binary vectors as a trade-off process. Note that the memory footprint of conventional row-wise quantization techniques is dominated by the size of binary vectors because the size of scaling factors is usually ignorable if the column width of a matrix is large enough. Compared to the conventional scheme, our proposed group-wise BCQ provides a new wide search space for quantization formats to meet a target compression ratio. Fig. 4 shows an example with two (g, q) configurations to quantize an (8×8) matrix. Indeed, even if the number of quantization bits is smaller, the memory footprint can be large when the group size g is small (i.e., more scaling factors are employed).

c) *Exploration of Compression Ratio:* To study the capability of group-wise BCQ to enlarge search space for com-

pression, we conduct experiments using GPT-2 Medium², GPT Neo³ 1.3B and 2.7B whose pre-trained models are publicly available. Specifically, we apply post-training quantization (with an iterative solver introduced in [20]) to those three pre-trained models while g and q vary. Then, each quantized model is evaluated on the WikiText-2 dataset to obtain the perplexity (PPL) to find the relationship between compression ratio and PPL. Fig. 5 shows PPL degradation and compression ratio⁴ when we try various q values (from 3 to 6) and g values (from 8 to matrix column width (i.e., row-wise)). From Fig. 5, we observe that the relationship between PPL degradation and g are vastly different depending on q . As a result, compared to the conventional row-wise quantization, group-wise BCQ offers new optimal configurations. For example in the case of the GPT-2 Medium model in Fig. 5, when a target PPL degradation is around 4.0, then 4-bit quantization is superior to 3-bit quantization in terms of compression ratio (even though g values are different). Thus, for a target PPL degradation (or a target compression ratio), we need to explore various q and g values simultaneously to achieve the best compression ratio (or the minimum PPL degradation). Note that for GPT Neo 1.3B and 2.7B, as we discussed the limits of row-wise quantization for large-scale LMs, a small g value is critical to achieving low PPL degradation. All in all, the effects of q and g on accuracy differ with each model such that q and g are hyper-parameters to be optimized.

Fig. 6 describes PPL (of four GPT-2 models with different sizes and one GPT Neo model) when diversified model sizes for each model are available by exploring q and g values. Even though we adopt post-training quantization instead of quantization-aware training (that might be too expensive for recent large LMs), the sizes of all 5 models in Fig. 6 are reduced a lot by our group-wise quantization. Suppose that we can tolerate some reasonable PPL degradation, we notice that larger models tend to be compressed by a higher compression ratio, which is consistent with a report in [35]. In the next subsections, we study a matrix multiplication kernel to facilitate the potential benefits of group-wise BCQ formats.

B. Quantized Matrix Multiplication based on Lookup Tables

Under our quantization scheme that quantizes weights by using BCQ format and maintains activations to be full-precision, naive matrix multiplications result in duplicate and redundant partial computations. To illustrate, assume that a binary matrix $\mathbf{B} \in \{-1, +1\}^{4 \times 4}$ and an activation vector $\mathbf{x} \in \mathbb{R}^4$ are given as

$$\mathbf{B} = \begin{bmatrix} +1 & -1 & -1 & +1 \\ +1 & -1 & +1 & -1 \\ +1 & -1 & -1 & -1 \\ -1 & +1 & -1 & +1 \end{bmatrix}, \quad \mathbf{x}^\top = \begin{bmatrix} 1.2 \\ -0.7 \\ 0.3 \\ 0.6 \end{bmatrix}. \quad (2)$$

Then, computing $\mathbf{B}\mathbf{x}^\top$ (that is to be multiplied by scaling factors) would repeat $(1.2 - (-0.7))$ three times and $(-0.3 +$

²<https://huggingface.co/gpt2-medium>

³<https://huggingface.co/EleutherAI>

⁴Calculated as FP32 model size divided by each quantized model size.

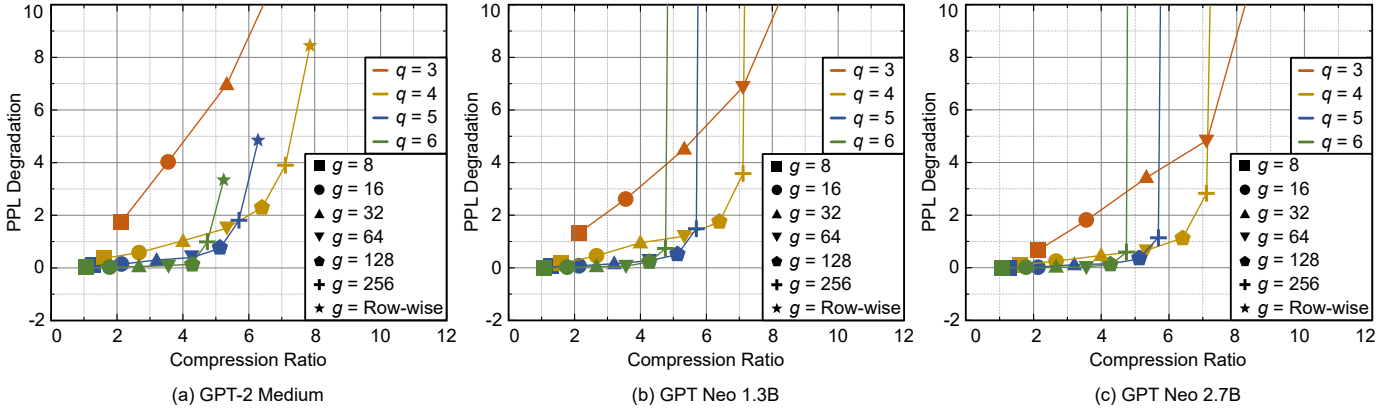


Fig. 5. PPL degradation and compression ratio with the various number of quantization bits (q) and group size (g). Three pre-trained models are quantized (by post-training quantization method) and then evaluated on the WikiText-2 dataset.

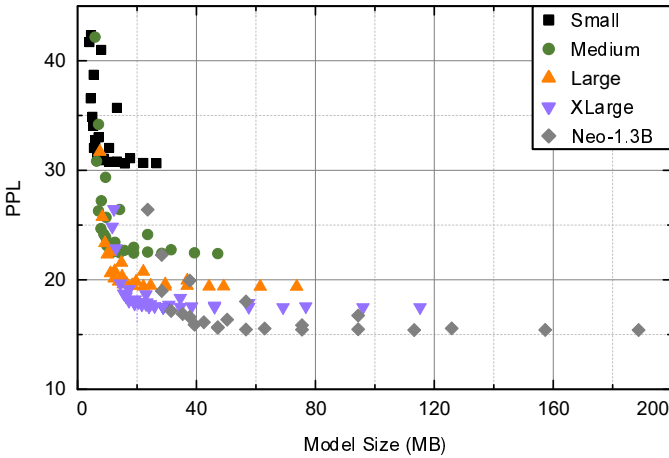


Fig. 6. PPL of GPT-2 models and a GPT Neo model when various model sizes for each model are attainable by q and g exploration.

TABLE II
EXAMPLE OF A LOOKUP TABLE TO STORE PRE-COMPUTED VALUES WITH A SUB-VECTOR OF \mathbf{x} WHEN $\mu=3$.

Binary Patterns	Key	Value
$\{-1, -1, -1\}$	0 (b'000)	$-x_1 - x_2 - x_3$
$\{-1, -1, +1\}$	1 (b'001)	$-x_1 - x_2 + x_3$
$\{-1, +1, -1\}$	2 (b'010)	$-x_1 + x_2 - x_3$
$\{-1, +1, +1\}$	3 (b'011)	$-x_1 + x_2 + x_3$
$\{+1, -1, -1\}$	4 (b'100)	$+x_1 - x_2 - x_3$
$\{+1, -1, +1\}$	5 (b'101)	$+x_1 - x_2 + x_3$
$\{+1, +1, -1\}$	6 (b'110)	$+x_1 + x_2 - x_3$
$\{+1, +1, +1\}$	7 (b'111)	$+x_1 + x_2 + x_3$

0.6) two times. Such redundant computations are caused by digitized elements of \mathbf{B} , and thus, we expect more duplicated computations as the size of matrices increases according to the growth of model size. Moreover, loading each element of \mathbf{B} requires bi-level memory accesses that can be slow for commercial CPUs and GPUs.

To avoid bit-level memory accesses and perform $\mathbf{B}\mathbf{x}^\top$ efficiently, we can pre-compute all possible combinations of full-precision activations and binary patterns. Note that a lookup

table (LUT) has been widely used to save processing time when numerous computations yield outputs within a restricted set [36]–[38]. LUT-based computation is justified especially when retrieving a value from a LUT is much faster than carrying out the original calculations. BCQ format (without quantizing activations that require heavy modifications in training codes and model structure [23], [25]) is also useful to be implemented by LUT-based approaches. For example, with every 3 elements $\{x_1, x_2, x_3\}$ in \mathbf{x} , we can pre-compute 8 ($=2^3$) possible values as shown in Table II and store those values in a LUT. Let μ be the length of a sub-vector of \mathbf{x} to construct a LUT (hence, μ is 3 in Table II). Once 2^μ values of a LUT are generated by using a sub-vector of \mathbf{x} , arithmetic operations to obtain partial dot products (of $\mathbf{B}\mathbf{x}^\top$) are replaced with LUT retrieval operations while a key is given by concatenating μ binary elements of \mathbf{B} . To complete $\mathbf{B}\mathbf{x}^\top$ computation, as the final step, those partial products are summed and then multiplied by scaling factors. When the row dimension of \mathbf{B} is enlarged (as generative LMs get larger), the utilization of a LUT increases due to more occurrences of redundant computations.

Let us briefly explain how to optimize μ that is also discussed in [19]. If μ increases, LUT construction cost increases as well by 2^μ . Such increased μ , however, can enhance computational parallelism because we can replace the μ number of FP32 additions with one LUT retrieval operation. Thus, as reported in [19], there exists an optimal μ to maximize the speed-up. Note that optimizing μ also needs to consider aligned memory accesses. In our work, $\mu = 8$ is used as a practical choice.

C. nuQmm for Group-Wise BCQ Format

In addition to the LUT-based scheme (eliminating redundant computations and bit-level memory accesses), our proposed nuQmm needs to achieve high performance with group-wise quantization in order to enhance accuracy for a given q . Targeting single-batch operations on GPUs, we propose the following as our strategy:

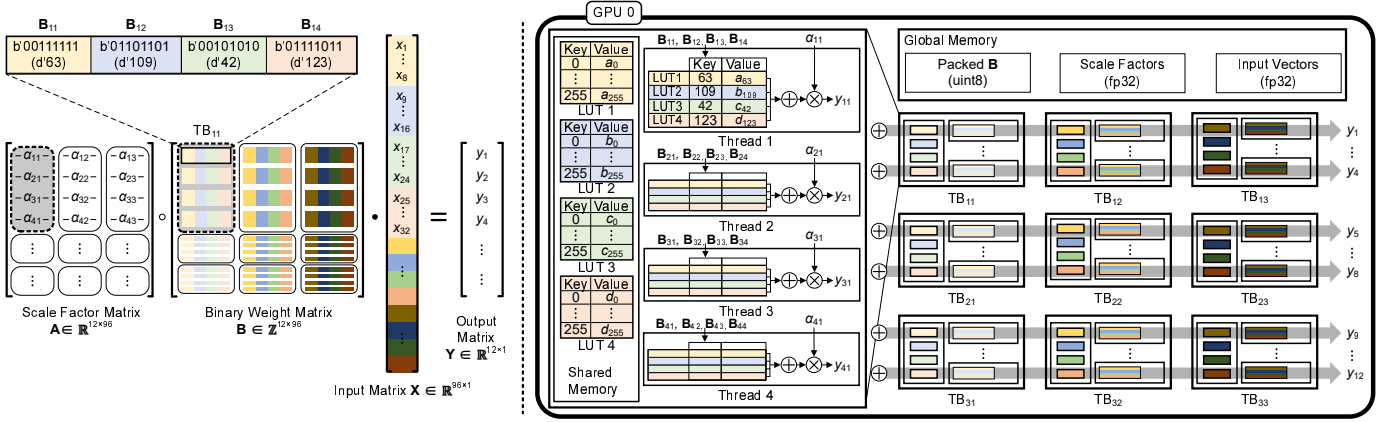


Fig. 7. The overview of nuQmm implementation on GPUs. In this example, we assume $m = 12$, $n = 96$, $\mu = 8$, $t_h = 4$, $l = 4$, $t_w = 32$, $q = 1$, and $g = 32$. “ \circ ” denotes element-wise multiplication and “ \cdot ” indicates a tensor product.

- To improve parallelism, we create as many threads as possible while each thread is allowed to perform independent LUT accesses.
- Binary weights accessed by a thread can share a common scaling factor such that operations related to scaling factors do not degrade the performance of a thread.
- If we allocate too small resources to a thread, then LUT utilization can be low and synchronization overhead can increase. As such, we need to optimize thread configurations empirically.

For the sake of simplicity, we formulate the proposed group-wise quantized matrix multiplication as $\mathbf{y} = \sum_{i=1}^g (\mathbf{A}_i \circ (\mathbf{B}_i \cdot \mathbf{x}))$, where \mathbf{A} is an $(m \times n)$ FP32 scaling matrix, \mathbf{B} is an $(m \times n)$ FP32 binary matrix, \mathbf{x} is an FP32 input vector of size n , and the operator \circ indicates element-wise multiplication. Note that in real situations, the memory footprint of \mathbf{A} is reduced by g since every g weights share a scaling factor.

a) *Overall Architecture*: For nuQmm, we assign l number of LUTs to a thread block (TB) of GPU. Then, the size of submatrix of \mathbf{A} and \mathbf{B} allocated to each TB becomes $(t_h \times t_w)$ when $t_w = l \times \mu$. Small t_h can increase the number of available threads while large t_h enhances LUT utilization inside a TB. Thus, t_h is empirically determined (2048 is a practical number for large-scale LMs). Note that the amount of resources allocated to each TB is small enough such that multiple TBs can share a scaling factor as long as g is larger than $l \times \mu$. The overall nuQmm implementation scheme on GPUs is presented in Fig. 7 when we assume $\mu = 8$, $l = 4$, $t_w = 32$, $t_h = 4$, $q = 1$, and $g = 32$. For $q > 1$, the entire process of Fig. 7 can be iterated q times while intermediate results are accumulated.

b) *Detailed Implementation*: Each TB first conducts pre-computation using partial x values assigned in order to fill up the l number of LUTs. Then l LUTs can be shared by all threads inside a TB (so as to mitigate costly global memory accesses) and multiple rows of a submatrix of \mathbf{B} can be processed by multiple threads (so as to improve throughput).

TABLE III
COMPARISON BETWEEN FP32 GEMM IN cuBLAS AND NUQMM. AN $(m \times n)$ MATRIX IS MULTIPLIED BY $(n \times 1)$ MATRIX AS AN SINGLE-BATCH OPERATION.

$m = n$	q	Memory (MB)		Latency (μs)	
		cuBLAS	nuQmm (Reduction)	cuBLAS	nuQmm (Speed up)
2048	2		1.06 (x15.9)		9.54 (x3.2)
	3		1.58 (x10.6)		10.23 (x3.0)
	4	16.78	2.11 (x8.0)	30.99	10.93 (x2.8)
	5		2.63 (x6.4)		11.43 (x2.7)
4096	2		4.21 (x15.9)		15.17 (x5.8)
	3		6.31 (x10.6)		17.35 (x5.1)
	4	67.11	8.40 (x8.0)	88.01	20.98 (x4.2)
8192	2		16.81 (x16.0)		37.65 (x8.3)
	3		25.20 (x10.7)		44.94 (x7.0)
	4	268.44	33.59 (x8.0)	313.22	52.06 (x6.0)
12288	2		37.80 (x16.0)		73.45 (x9.5)
	3		56.67 (x10.7)		84.45 (x8.3)
	4	603.98	75.55 (x8.0)	697.85	99.93 (x7.0)
	5		94.42 (x6.4)		117.67 (x5.9)

When threads finish retrieving and summing LUT values, scaling factors are fetched (only once for each thread) and multiplied to produce partial outputs. Finally, $\frac{n}{l \times \mu}$ partial outputs are accumulated across TBs (through `atomicAdd` operations, as illustrated in Fig. 7) to generate the final outputs. LUTs are stored in shared memory inside GPU and the shared memory presents high bandwidth (e.g., 17TB/s for RTX-3090). Thus, high memory accesses for LUTs (while multiple FLOPs can be replaced with one LUT access) enable fast matrix computations. As for memory size of LUTs, only 1KB is required for every 8 hidden dimensions and the shared memory size is more than a few megabytes (e.g., 10MB for RTX-3090 with 128KB per SM and 82 SMs available). Thus, the whole LUTs can be safely stored in shared memory. To illustrate, the hidden dimension can be up to 80,000 for RTX-3090 while 16,384 is the hidden dimension for GPT-3 175B.

Table III compares memory footprint and latency between conventional FP32 GEMM kernel in cuBLAS library and our

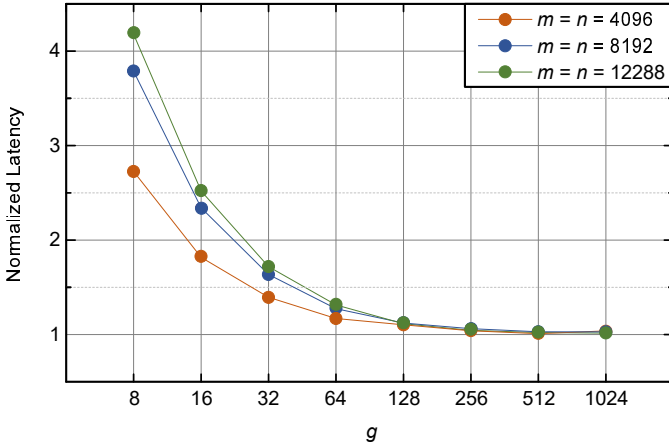


Fig. 8. Normalized matrix multiplication latency when a $(m \times n)$ weight matrix is quantized by $(q=4)$ bits with different g values.

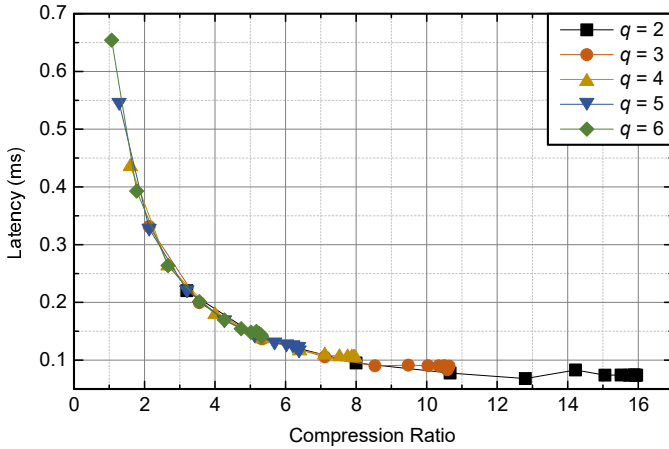


Fig. 9. Relationship between latency and compression ratio when nuQmm performs quantized matrix multiplications with $m = 12288$ and various (q, g) pairs.

proposed nuQmm. For experiments, we multiply an $(m \times n)$ matrix (that can be quantized by q bits) and an $(n \times 1)$ matrix using a single Nvidia 3090 GPU with CUDA 11.5. We can observe that the memory size and execution time required for both cuBLAS and nuQmm increase with larger m (and q for nuQmm). It is clear that the relative reduction of memory footprint and latency by nuQmm increases when a larger weight matrix is employed. Such observation can be partly explained by the fact that kernel launch overhead appears as a performance bottleneck for small matrices (such as $m = 2048$). Thus, the merits of nuQmm would be outstanding as larger-scale generative LMs are introduced.

To examine latency variance of nuQmm on group size g , we perform matrix multiplications (using an $(m \times n)$ matrix and an $(n \times 1)$ matrix) when g values vary. In Fig. 8, for each $m (= n)$ selection, matrix multiplication latency of different g is compared with that of row-wise (i.e., $g = n$) BCQ format. Interestingly, when $g > 64$, group-wise nuQmm is as fast as row-wise nuQmm regardless of m in Fig 8. In other words,

a reasonably large g (such as 256 and 512) can result in fast nuQmm while accuracy improvement by group-wise is substantial as can be seen in Fig. 5.

To understand the underlying mechanisms in Fig. 8, we analyze memory footprint of nuQmm because single-batch operations are basically memory-bound such that latency is proportional to memory footprint. Let S_b and S_α represent space complexity of binary weights and scaling factors, respectively. Then the overall space complexity S can be described as

$$\begin{aligned}
 S &= S_b + S_\alpha = \mathcal{O} \left(1 \cdot m \cdot n \cdot q + 32 \cdot m \cdot \frac{n}{g} \cdot q \right) \\
 &= \mathcal{O} \left(m \cdot n \cdot q \left(1 + \frac{32}{g} \right) \right).
 \end{aligned} \tag{3}$$

As a consequence, if $g \gg 32$, S can be independent of g and approximated to be $\mathcal{O}(m \cdot n \cdot q)$. To verify our claim that latency of nuQmm is proportional to memory footprint (when running single-batch operations), we explore various (q, g) pairs and compression ratios correspondingly, and measure matrix multiplication latency when $m = 12288$ as shown in Fig. 9. It can be noticed that the additional search parameter g allows a fine-grained search space of compression ratio that is not available by q alone. Across all available compression ratios in Fig. 9, latency is a function of compression ratio. For instance, if two different pairs (q_1, g_1) and (q_2, g_2) exhibit a similar memory footprint, then we can expect similar latency by nuQmm.

D. Comparison with Tensor Parallelism (of Full-Precision)

Since the model size is rapidly increasing in order to empower language models to improve accuracy on various tasks, computing systems are scaled up with a growing number of computation units and memory capacity. Note that for highly parallel computing systems, such as GPUs, high memory bandwidth is essential to feed lots of arithmetic units so as to maintain high resource utilization. The main memory system of GPUs, hence, is inclined to focus on high bandwidth instead of large capacity. Correspondingly, even though new innovative memory architectures (e.g., HBM [39]) are proposed, the maximum memory capacity for a single GPU is still limited up to a few tens of gigabytes [16]. Such limited GPU's memory capacity derived various parallelism ideas to partition a large-scale LM over multiple GPUs [13], [14]. In this work, we consider tensor parallelism that can split matrix multiplications over multiple GPUs, which is useful for both training and inference. Note that even though tensor parallelism can generate smaller sub-tasks that can be executed simultaneously, synchronization and GPT-to-GPU communication overhead are additionally induced. Our new BCQ format and nuQmm can reduce the model size with low latency such that the overhead of tensor parallelism can be alleviated.

For a comparison between nuQmm and cuBLAS, we measure the latency of completing a large matrix multiplication as

TABLE IV

PROFILING RESULTS OF MATRIX MULTIPLICATIONS (WITH AN $(m \times m)$ MATRIX AND AN $(m \times 1)$ MATRIX). FOR NUQMM, $g = m$ AND q IS 2 OR 4.

Type	GPUs	m	Comput. Ratio (%)	Comm. Ratio (%)	Speed up	GPU Util. (%)	Memory Util. (%)	Average Power (W)	Total Energy (mJ)	Normalized Energy
cuBLAS	1	8192	100.00	0.00	1.00	96.67	100.00	318.33	99.80	1.00
cuBLAS	2	8192	84.55	15.45	1.54	88.06	92.46	321.06	130.77	1.31
cuBLAS	4	8192	68.84	31.16	1.95	72.82	59.73	260.78	168.14	1.68
cuBLAS	8	8192	55.23	44.77	1.73	55.25	26.92	197.01	286.50	2.87
nuQmm ($q = 2$)	1	8192	100.00	0.00	8.33	85.85	69.90	333.78	12.57	0.13
nuQmm ($q = 4$)	1	8192	100.00	0.00	5.90	90.85	82.89	331.97	17.64	0.18
cuBLAS	1	12288	100.00	0.00	1.00	97.37	100.00	317.90	221.59	1.00
cuBLAS	2	12288	90.44	9.56	1.76	93.38	99.79	320.57	254.41	1.15
cuBLAS	4	12288	80.56	19.44	2.46	83.29	81.40	310.75	351.49	1.59
cuBLAS	8	12288	61.65	38.35	2.98	64.59	45.33	239.83	448.29	2.02
nuQmm ($q = 2$)	1	12288	100.00	0.00	12.21	91.36	91.35	331.21	18.91	0.09
nuQmm ($q = 4$)	1	12288	100.00	0.00	6.89	95.02	99.57	327.07	33.10	0.15
cuBLAS	1	16384	100.00	0.00	1.00	98.16	100.00	317.83	387.72	1.00
cuBLAS	2	16384	93.15	6.85	1.77	94.60	100.00	321.13	435.48	1.12
cuBLAS	4	16384	84.04	15.96	3.06	89.86	94.40	319.52	510.66	1.32
cuBLAS	8	16384	69.01	30.99	3.89	72.83	60.33	263.67	663.54	1.71
nuQmm ($q = 2$)	1	16384	100.00	0.00	13.41	93.92	99.20	329.24	29.95	0.08
nuQmm ($q = 4$)	1	16384	100.00	0.00	7.43	96.94	100.00	327.98	53.88	0.14

shown in Fig. 10. We assume that we multiply an $(m \times m)$ matrix and an $(m \times 1)$ matrix (as a single-batch operation to run inference of generation steps in Fig. 1) when m can be 4096, 8192, or 16384. For conventional full-precision (FP32) cuBLAS [11], one to eight GPUs serve tensor parallelism through NCCL library [16] to communicate via PCIe 4.0. When nuQmm is applied (with only one GPU), q is given as 4 and g is the same as m^5 . From Fig. 10, we observe the following: 1) for cuBLAS, more GPUs with tensor parallelism can reduce the overall computation latency while communication latency increases, 2) tensor parallelism is more effective with larger m , and 3) for all three m configurations, nuQmm is faster than cuBLAS even 8 GPUs are employed. Note that if m is small, then communication latency (including GPU-to-GPU communication and synchronization across GPUs) cannot be ignored. As such, latency improvement by tensor parallelism is a sub-linear function of the number of GPUs (for any m) such that certain configurations of tensor parallelism may even harm the overall inference latency (while the cost of inference system increases due to more GPUs). In the case of nuQmm, the requirement for tensor parallelism can be eliminated (or alleviated) due to reduced model size. As a result, nuQmm can reduce both latency and system design cost of inference.

Table IV is a summary of profiling results of matrix multiplications performed by using cuBLAS (with tensor parallelism) or nuQmm (with one GPU). In this work, GPU power and other metrics are collected by using *nvidia-smi* utility [40], [41]. Again, an $(m \times m)$ matrix is multiplied by an $(m \times 1)$ matrix while we select m to be 8192, 12288 (used for GPT-3 175B), or 16384. For Table IV, we include the case of $q = 2$ for nuQmm (with $g = m$) as 2-bit quantization for the Transformer is reported to be feasible by quantization-aware training along with BCQ format [30]. We notice that throughout all m configurations, increasing

⁵As shown in Fig. 8, unless g is too small, g does not affect latency noticeably. Thus, we show row-wise quantization results in this section.

GPUs for cuBLAS with tensor parallelism brings about a higher reduction in GPU utilization, memory utilization, and latency ratio of computations. As evidenced by the increase in the latency ratio of communication, such reductions in utilization indicate that some GPUs can be temporarily idle until all GPUs are synchronized. Accordingly, the amount of speed-up that can be obtained by tensor parallelism is a lot smaller than the number of GPUs. As a result, cuBLAS with more GPUs causes increased energy consumption for matrix multiplications. On the other hand, nuQmm (with one GPU) can offer high speed-up (that cannot be achieved by tensor parallelism) while retaining high GPU/memory utilization. Combining low latency and a reduced number of GPUs, thus, nuQmm saves energy consumption for matrix multiplications significantly. For example, when $m = 12288$, nuQmm (with $q = 2$) achieves $11.7\times$ energy reduction and $12.2\times$ speed-up compared to cuBLAS with one GPU.

IV. EXPERIMENTAL RESULTS ON GPT-3 175B

In this section, we apply nuQmm to major matrix multiplications in GPT-3 175GB [6] (chosen as a representative large-scale LM) and estimate speed-up and energy reduction. GPT-3 follows the structure of the Transformer [5] that consists of identical layers. Assuming that m is the hidden size (i.e., d_{model}), each layer has multi-head attention and feed-forward network as shown in Fig. 11 and includes 4 major linear computations of higher time complexity (than the other non-linear operations) for which we multiply a $(m \times 1)$ activation matrix and the following 4 matrices:

- $(m \times m)$ matrix for attention output
- $(3m \times m)$ matrix for key, query, and value of attention
- $(m \times 4m)$ matrix for the first feed-forward sub-layer
- $(4m \times m)$ matrix for the second feed-forward sub-layer

Since all layers of the Transformers have identical structures and matrix multiplications dominate the entire inference latency [30], we can successfully approximate the overall impact

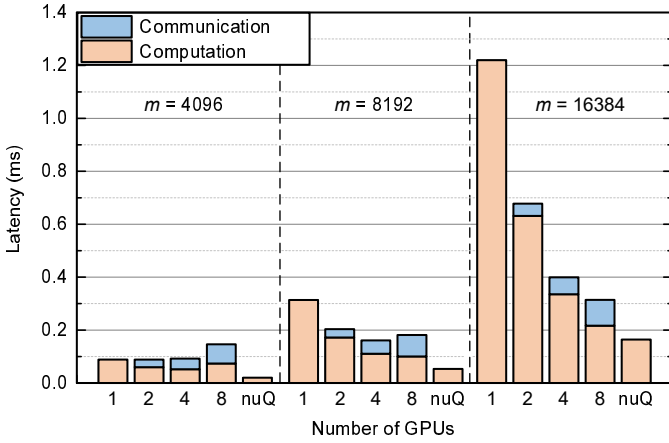


Fig. 10. Latency comparison between full-precision cuBLAS and nuQmm. We multiply an $(m \times m)$ matrix and $(m \times 1)$ matrix (for single-batch inference). For cuBLAS, tensor parallelism is utilized with up to 8 GPUs. For nuQmm, q and g are 4 and m , respectively.

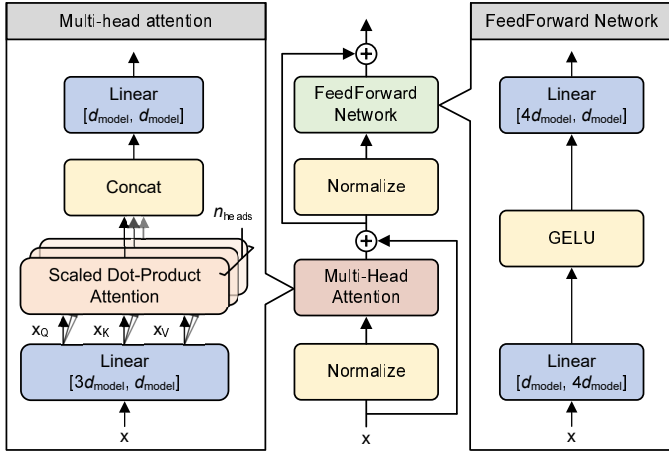


Fig. 11. Transformer layer incorporating multi-head attention and feed-forward network performing 4 major matrix multiplications.

of nuQmm on a generative LM by estimating speed-up and energy reduction using the above 4 matrix multiplications.

By setting m to be hidden dimension size 12288 of GPT-3 175B, Table V compares speed-up and energy reduction between cuBLAS (1 or 8 GPUs) and nuQmm (q is 2 or 4). It should be noted that even though we include the result of FP32 cuBLAS with one GPU, the entire parameters of GPT-3 175B cannot be stored in the main memory of one GPU. Thus, multiple GPUs would be mandatory if we do not quantize GPT-3 175B. We can observe that for all matrix multiplications in Table V, nuQmm presents high performance with less energy consumption. Even though we present a few matrix configurations Table V, such matrix configurations are repeatedly presented through Transformer blocks of the same structure. Thus, Table V is useful to estimate the overall performance improvement of GPT models as m increases or nuQmm is applied. Overall, the total speed-up and energy reduction of GPT-3 175B by nuQmm (with $q = 2$) can be approximated to be $14.4\times$ and $14.3\times$, respectively, compared

TABLE V
SPEED-UP AND ENERGY REDUCTION BY NUQMM ON GPT-3 175B FOR WHICH m IS SET TO BE HIDDEN DIMENSION SIZE 12288.

Layer Type (Shape)	Kernel	GPUs	q	Speed-up	Norm. Energy
Attention query,key,value ($3m, m$)	cuBLAS	1	(FP32)	1.00	1.00
	cuBLAS	8	(FP32)	4.18	1.65
	nuQmm	1	2	14.29	0.07
	nuQmm	1	4	7.47	0.14
Attention output (m, m)	cuBLAS	1	(FP32)	1.00	1.00
	cuBLAS	8	(FP32)	3.00	2.02
	nuQmm	1	2	12.25	0.09
	nuQmm	1	4	6.88	0.15
FFN 1st sub-layer ($m, 4m$)	cuBLAS	1	(FP32)	1.00	1.00
	cuBLAS	8	(FP32)	5.65	1.38
	nuQmm	1	2	15.04	0.07
	nuQmm	1	4	7.80	0.13
FFN 2nd sub-layer ($4m, m$)	cuBLAS	1	(FP32)	1.00	1.00
	cuBLAS	8	(FP32)	4.70	1.47
	nuQmm	1	2	14.54	0.07
	nuQmm	1	4	7.41	0.14
Total (Attention + FFN)	cuBLAS	1	(FP32)	1.00	1.00
	cuBLAS	8	(FP32)	4.59	1.53
	nuQmm	1	2	14.41	0.07
	nuQmm	1	4	7.50	0.14

to cuBLAS with 1 GPU (or $3.2\times$ and $21.9\times$, respectively, compared to cuBLAS with 8 GPUs). In our experiments, we do not consider uniform quantization because 1) at least 8 bits are necessary for the Transformers [27], [28], [30], 2) activations need to be dynamically quantized during inference with quantization/dequantization overhead, and 3) to the best of our knowledge, uniform quantization for generative LMs has not been reported.

V. EXTENSION OF NUQMM FOR GENERATIVE LMS

In this section, we discuss additional architectural considerations for nuQmm to be extensively useful for various generative language models.

A. Mixed Precision using nuQmm

It is well known that different layers of neural networks present different sensitivity to model compression [42], [43]. For example, parameter pruning acquires various pruning rates for layers given a target global pruning rate and test accuracy [44], [45]. As such, mixed precision techniques for quantization are eligible for obtaining higher compression ratio practical techniques by assigning different quantization bits to layers while measuring accurate sensitivity of layers is complicated and computationally demanding [42], [46]. Note that since we introduce an additional parameter g (i.e., group size for scaling factors), nuQmm can offer wider search space exploration for mixed precision compared to the conventional methods allowing the number of quantization bits as the only search parameter.

For experiments, we consider two sub-layers (multi-head attention and feed-forward networks) in Fig. 11 to be quantized by different quantization schemes with nuQmm. In order to facilitate efficient exploration of search space for mixed precision, we set the following constraints: 1) all matrices of

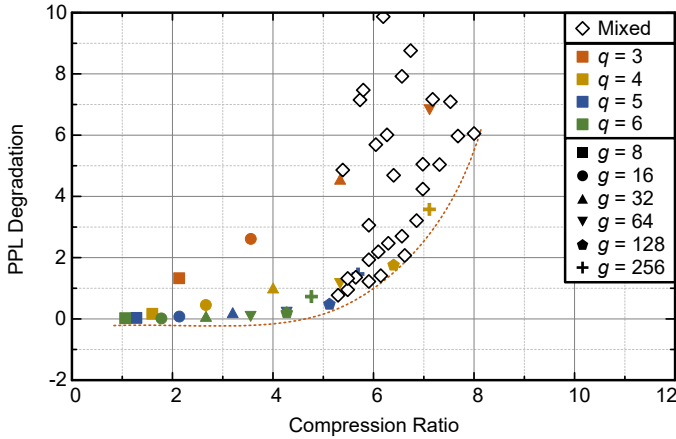


Fig. 12. Mixed precision quantization results using GPT Neo 1.3B. All matrices of the same sub-layer type are quantized by the same (q, g) configuration. Available sets for exploring q and g are $\{3, 4, 5\}$ and $\{128, 256, 512, 2048\}$, respectively.

each sub-layer type (i.e., multi-head attention or feed-forward network) across all layers are quantized by the same (q, g) configuration, 2) q is selected to be one of $\{3, 4, 5\}$, and 3) g is selected to be one of $\{128, 256, 512, 2048\}$ that lead to less than 10% latency overhead compared to row-wise quantization as depicted in Fig. 8.

Fig. 12 shows PPL degradation of GPT Neo 1.3B quantized by mixed precision (using two (q, g) configurations as described above) in addition to the previous quantization results of Fig. 5 that allow only one (q, g) configuration across all layers. Notice that mixed precision combined with additional parameter g produces extensive trade-offs between PPL degradation and compression ratio. Due to our selected ranges for q and g , we extract numerous (q, g) pairs enabling high compression ratio with reasonable PPL degradation in Fig. 12. Further optimal points would be obtainable by fine-grained mixed precision with more diversified (q, g) configurations for layers and matrices at the cost of additional evaluation time.

B. Context Processing using Quantized Weights

As we discussed, inference of generative LMs can be separated into the summarization stage (using input context) and the generation stage as shown in Fig. 2. Note that even though the same weights can be applied to both summarization and generation, those two processes require different batch sizes. As for summarization, since tokens for input context are already provided, multiple tokens can be fed into the Transformer to improve explicit parallelism. On the other hand, the generation stage is fundamentally processed by single-batch operations because of autoregressive properties. In other words, inference of generative LMs is basically supposed to support two potentially conflicting operations, namely, compute-bound context process with high parallelism and memory-bound generation process with low parallelism.

Because nuQmm is specifically designed for single-batch matrix multiplications, the context process can be better performed by conventional kernels with parallel computing

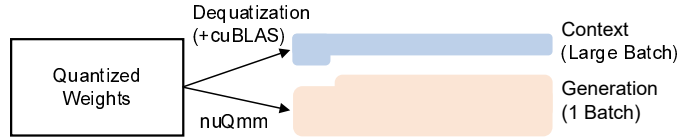


Fig. 13. Our proposed strategy to support both context process and generation process using quantized weight with BCQ format.

resources (such as Tensor Cores of Nvidia [31]). As such, we propose our inference strategy as shown in Fig. 13. Quantized weights are stored in memory in the form of BCQ and then 1) dequantized to conduct full-precision cuBLAS matrix multiplications for context process or 2) used as inputs of nuQmm for the generation process. The rationale behind our approach is as follows:

- It is necessary to quantize weights even for the context process. Otherwise, the effort to save memory by nuQmm would be worthless.
- Dequantization overhead (in latency) becomes ignorable as more tokens are utilized for context process and/or generation process.
- If input context gets longer, then the latency of cuBLAS matrix multiplications is a lot higher than that of dequantization (due to higher time complexity).
- As target tasks require more tokens to be generated, the generation stage would dominate inference latency (and then, the latency of the entire context process including dequantization can be negligible).

Few-shot learning or in-context learning techniques first introduced in GPT-3 [6] intentionally require a small number of tokens for context.

VI. DISCUSSION

In this paper, we consider the FP32 format as a baseline for various comparisons with the BCQ format. Admittedly, low-precision formats are actively studied because well-trained neural networks (with proper regularization) can be robust to various noise sources. As an example, BFLOAT16 [47] has 16 bits to represent a parameter, and thus, saves memory footprint and area overhead of arithmetic units compared to FP32. Recently, large-scale generative models (e.g., [6], [9], [13]) are developed by mixing BFLOAT16 and FP32. Specifically, BFLOAT16 is selected for major matrix multiplications while FP32 is utilized to perform various non-linear operations (such as normalization layers, SoftMAX, and activation functions). Compared to FP32, BFLOAT16 can halve memory bandwidth and offer double peak performance. Thus, our estimated speed-up and energy savings by nuQmm can be roughly reduced by 50% while such improvements are still significant.

For our experiments, we measured the accuracy of quantized models by performing a post-training quantization method for fast design exploration of nuQmm. There are several ways to further improve accuracy and/or compression ratio. For example, quantization-aware training for Transformers [30] is reported to save additional 1 or 2 quantization bits

at the cost of training time with hyper-parameter tuning. In particular to self-supervised language models, fine-tuning techniques (e.g., LoRA [48]) using a small dataset can be a potentially economic choice to improve accuracy after post-training quantization. Applying nuQmm to such advanced quantization techniques is left as future works.

Pre-trained extreme-scale language models (e.g., GPT-3 (175B) [6], HyperCLOVA (204B) [8], and Megatron Turing NLG (530B) [10]) are usually not publicly available. Thus, in this work, our detailed analysis of group-wise quantization and nuQmm is limited to relatively smaller models (such as GPT Neo). In the case of GPT-3 175B, since it is not feasible to find q for reasonable model accuracy without a pre-trained model, we assumed $q = 2$ or $q = 4$ to estimate speed-up and energy consumptions of major matrix multiplications based on the reports that larger neural networks can be quantized by a smaller number of quantization bits [21], [49].

The parameter pruning technique is a promising complement to parameter quantization in order to further compress neural networks [43], [50]. When parameters identified as unimportant are removed first, then quantization can be performed with a reduced number of parameters. Then, the number of quantization bits can also be reduced along with a smaller quantization error [51]. Both fine-grained pruning and structured pruning are investigated because of trade-offs between compression ratio and the regularity of memory access patterns [12], [52]. Exploring pruning techniques to integrate nuQmm with proper sparse representation (to be practical with GPUs or CPUs) would be interesting.

VII. CONCLUSION

Generative language models, such as GPT-3 175B, are attracting attention due to their generation capability on various complicated tasks. It is widely expected that the growth rate in parameter size would be exponential to follow scaling laws in natural language processing. The inference speed, however, is a serious concern not only because of parameter size increase but also because of autoregressive operations associated with single-batch operation. Thus, conventional matrix multiplication using cuBLAS leads to low utilization of GPUs and low performance during the running of the generation stage of the Transformer decoder.

To improve the inference speed of large-scale generative models, in this paper, we proposed a new group-wise binary-coding quantization format and a dedicated matrix multiplication kernel nuQmm. By introducing a new hyper-parameter, group size, it is possible to explore a wider compression ratio such that conventional row-wise quantization is replaced with our group-wise quantization. Then, LUT-based matrix multiplication enables computations with quantized weights without a special conversion process. As such, our nuQmm can exploit both low latency and reduced memory footprint. nuQmm is especially superior to tensor parallelism that is required if a model size is too big to be accommodated in a single GPU. Combining low latency and a reduced number of GPUs, inference of GPT-3 175B can be performed with

significantly reduced energy consumption. We also discussed additional considerations of nuQmm such as mixed precision and context processing.

REFERENCES

- [1] J. Devlin, M.-W. Chang, K. Lee, and K. Toutanova, "BERT: Pre-training of deep bidirectional transformers for language understanding," in *Proceedings of the 2019 Conference of the North American Chapter of the Association for Computational Linguistics: Human Language Technologies, Volume 1 (Long and Short Papers)*, 2019, pp. 4171–4186.
- [2] W. Hu, B. Liu, J. Gomes, M. Zitnik, P. Liang, V. Pande, and J. Leskovec, "Strategies for pre-training graph neural networks," in *International Conference on Learning Representations*, 2020.
- [3] A. Baevski, Y. Zhou, A. Mohamed, and M. Auli, "Wav2vec 2.0: A framework for self-supervised learning of speech representations," in *Advances in Neural Information Processing Systems*, vol. 33, 2020, pp. 12 449–12 460.
- [4] T. Chen, S. Kornblith, M. Norouzi, and G. Hinton, "A simple framework for contrastive learning of visual representations," in *International conference on machine learning*. PMLR, 2020, pp. 1597–1607.
- [5] A. Vaswani, N. Shazeer, N. Parmar, J. Uszkoreit, L. Jones, A. N. Gomez, E. Kaiser, and I. Polosukhin, "Attention is all you need," *Advances in neural information processing systems*, vol. 30, 2017.
- [6] T. Brown, B. Mann, N. Ryder, M. Subbiah, J. D. Kaplan, P. Dhariwal, A. Neelakantan, P. Shyam, G. Sastry, A. Askell *et al.*, "Language models are few-shot learners," *Advances in neural information processing systems*, vol. 33, pp. 1877–1901, 2020.
- [7] J. Kaplan, S. McCandlish, T. Henighan, T. B. Brown, B. Chess, R. Child, S. Gray, A. Radford, J. Wu, and D. Amodei, "Scaling laws for neural language models," *arXiv:2001.08361*, 2020.
- [8] B. Kim, H. Kim, S.-W. Lee, G. Lee, D. Kwak, J. D. Hyeon, S. Park, S. Kim, S. Kim, D. Seo *et al.*, "What changes can large-scale language models bring? intensive study on hyperclova: Billions-scale korean generative pretrained transformers," in *Proceedings of the 2021 Conference on Empirical Methods in Natural Language Processing*, 2021, pp. 3405–3424.
- [9] J. W. Rae, S. Borgeaud, T. Cai, K. Millican, J. Hoffmann, F. Song, J. Aslanides, S. Henderson, R. Ring, S. Young, E. Rutherford, T. Henighan, J. Menick, A. Cassirer, R. Powell, G. van den Driessche, L. A. Hendricks, M. Rauh, P.-S. Huang, A. Glaese, J. Welbl, S. Dathathri, S. Huang, J. Uesato, J. Mellor, I. Higgins, A. Creswell, N. McAleese, A. Wu, E. Elsen, S. Jayakumar, E. Buchatskaya, D. Budden, L. Sutherland, K. Simonyan, M. Paganini, L. Sifre, L. Martens, X. L. Li, A. Kuncoro, A. Nematzadeh, E. Gribovskaya, D. Donato, A. Lazaridou, A. Mensch, J.-B. Lespiau, M. Tsimpoukelli, N. Grigorev, D. Fritz, T. Sottiaux, M. Pajarskas, T. Pohlen, Z. Gong, D. Toyama, C. de Masson d'Autume, Y. Li, T. Terzi, V. Mikulik, I. Babuschkin, A. Clark, D. de Las Casas, A. Guy, C. Jones, J. Bradbury, M. Johnson, B. Hechtman, L. Weidinger, I. Gabriel, W. Isaac, E. Lockhart, S. Osindero, L. Rimell, C. Dyer, O. Vinyals, K. Ayoub, J. Stanway, L. Bennett, D. Hassabis, K. Kavukcuoglu, and G. Irving, "Scaling language models: Methods, analysis & insights from training gopher," *arXiv:2112.11446*, 2021.
- [10] S. Smith, M. Patwary, B. Norick, P. LeGresley, S. Rajbhandari, J. Casper, Z. Liu, S. Prabhumoye, G. Zerveas, V. Korthikanti *et al.*, "Using deepspeed and megatron to train megatron-turing nlg 530b, a large-scale generative language model," *arXiv preprint arXiv:2201.11990*, 2022.
- [11] S. Migacz, "8-bit inference with TensorRT," in *NVIDIA GPU Technology conference*, 2017.
- [12] J. Yu, A. Lukefahr, D. Palframan, G. Dasika, R. Das, and S. Mahlke, "Scalpel: Customizing DNN pruning to the underlying hardware parallelism," in *Proceedings of the 44th Annual International Symposium on Computer Architecture*, 2017, pp. 548–560.
- [13] M. Shoeybi, M. Patwary, R. Puri, P. LeGresley, J. Casper, and B. Catanzaro, "Megatron-lm: Training multi-billion parameter language models using model parallelism," *arXiv preprint arXiv:1909.08053*, 2019.
- [14] D. Narayanan, M. Shoeybi, J. Casper, P. LeGresley, M. Patwary, V. Korthikanti, D. Vainbrand, P. Kashinkunti, J. Bernauer, B. Catanzaro *et al.*, "Efficient large-scale language model training on gpu clusters using megatron-lm," in *Proceedings of the International Conference for High Performance Computing, Networking, Storage and Analysis*, 2021, pp. 1–15.
- [15] A. A. Awan, C.-H. Chu, H. Subramoni, and D. K. Panda, "Optimized broadcast for deep learning workloads on dense-gpu infiniband clusters: Mpi or ncl?" in *Proceedings of the 25th European MPI Users' Group Meeting*, 2018, pp. 1–9.
- [16] A. Li, S. L. Song, J. Chen, J. Li, X. Liu, N. R. Tallent, and K. J. Barker, "Evaluating modern gpu interconnect: Pcie, nvlink, nv-sli, nvswitch and gpudirect," *IEEE Transactions on Parallel and Distributed Systems*, vol. 31, no. 1, pp. 94–110, 2019.
- [17] S. Roy, J. Dean, S. Ghemawat, R. Sepassi, H. Lim, M. Isard, P. Barham, Y. Wu, L. Shafey, A. Chowdhery *et al.*, "Pathways: Asynchronous distributed dataflow for ml," *Proceedings of Machine Learning and Systems*, vol. 4, 2022.
- [18] N. Bell and M. Garland, "Efficient sparse matrix-vector multiplication on cuda," Tech. Rep., 2008.
- [19] Y. Jeon, B. Park, S. J. Kwon, B. Kim, J. Yun, and D. Lee, "Biggemm: matrix multiplication with lookup table for binary-coding-based quantized dnns," in *SC20: International Conference for High Performance Computing, Networking, Storage and Analysis*. IEEE, 2020, pp. 1–14.
- [20] C. Xu, J. Yao, Z. Lin, W. Ou, Y. Cao, Z. Wang, and H. Zha, "Alternating multi-bit quantization for recurrent neural networks," in *International Conference on Learning Representations (ICLR)*, 2018.
- [21] Y. Choi, M. El-Khamy, and J. Lee, "Towards the limit of network quantization," in *International Conference on Learning Representations (ICLR)*, 2017.
- [22] M. D. McDonnell, "Training wide residual networks for deployment using a single bit for each weight," in *International Conference on Learning Representations (ICLR)*, 2018.
- [23] B. Jacob, S. Kligys, B. Chen, M. Zhu, M. Tang, A. Howard, H. Adam, and D. Kalenichenko, "Quantization and training of neural networks for efficient integer-arithmetic-only inference," in *Proceedings of the IEEE Conference on Computer Vision and Pattern Recognition*, 2018, pp. 2704–2713.
- [24] R. Zhao, Y. Hu, J. Dotzel, C. D. Sa, and Z. Zhang, "Improving neural network quantization without retraining using outlier channel splitting," in *International Conference on Machine Learning (ICML)*, 2019, pp. 7543–7552.
- [25] S. Wu, G. Li, F. Chen, and L. Shi, "Training and inference with integers in deep neural networks," in *International Conference on Learning Representations (ICLR)*, 2018.
- [26] D. Lin, S. Talathi, and S. Annapureddy, "Fixed point quantization of deep convolutional networks," in *International Conference on Machine Learning*, 2016, pp. 2849–2858.
- [27] S. Kim, A. Gholami, Z. Yao, M. W. Mahoney, and K. Keutzer, "I-bert: Integer-only bert quantization," in *International conference on machine learning*. PMLR, 2021, pp. 5506–5518.
- [28] A. Bhandare, V. Sripathi, D. Karkada, V. Menon, S. Choi, K. Datta, and V. Saletore, "Efficient 8-bit quantization of transformer neural machine language translation model," *arXiv:1906.00532*, 2019.
- [29] M. Rastegari, V. Ordonez, J. Redmon, and A. Farhadi, "XNOR-Net: Imagenet classification using binary convolutional neural networks," in *ECCV*, 2016.
- [30] I. Chung, B. Kim, Y. Choi, S. J. Kwon, Y. Jeon, B. Park, S. Kim, and D. Lee, "Extremely low bit transformer quantization for on-device neural machine translation," in *Findings of the Association for Computational Linguistics: EMNLP 2020*, 2020, pp. 4812–4826.
- [31] S. Markidis, S. W. Der Chien, E. Laure, I. B. Peng, and J. S. Vetter, "Nvidia tensor core programmability, performance & precision," in *2018 IEEE international parallel and distributed processing symposium workshops (IPDPSW)*. IEEE, 2018, pp. 522–531.
- [32] T. Gale, M. Zaharia, C. Young, and E. Elsen, "Sparse gpu kernels for deep learning," in *SC20: International Conference for High Performance Computing, Networking, Storage and Analysis*. IEEE, 2020, pp. 1–14.
- [33] M. Nagel, R. A. Amjad, M. van Baalen, C. Louizos, and T. Blankevoort, "Up or down? adaptive rounding for post-training quantization," in *International Conference on Machine Learning (ICML)*, 2017, pp. 7696–7705.
- [34] Y. Guo, A. Yao, H. Zhao, and Y. Chen, "Network sketching: exploiting binary structure in deep CNNs," in *IEEE Conference on Computer Vision and Pattern Recognition (CVPR)*, 2017, pp. 4040–4048.
- [35] Z. Li, E. Wallace, S. Shen, K. Lin, K. Keutzer, D. Klein, and J. Gonzalez, "Train big, then compress: Rethinking model size for efficient training and inference of transformers," in *International Conference on Machine Learning*. PMLR, 2020, pp. 5958–5968.
- [36] P. K. Meher, "LUT optimization for memory-based computation," *IEEE Transactions on Circuits and Systems II: Express Briefs*, vol. 57, no. 4, pp. 285–289, 2010.
- [37] S. Xu, Q. Wang, X. Wang, S. Wang, and T. T. Ye, "Multiplication through a single look-up-table (LUT) in CNN inference computation,"

IEEE Transactions on Computer-Aided Design of Integrated Circuits and Systems, pp. 1–1, 2021.

- [38] R. de Queiroz and P. Stein, “LUT filters for quantized processing of signals,” *IEEE Transactions on Signal Processing*, vol. 52, no. 3, pp. 687–693, 2004.
- [39] S. Rajbhandari, O. Ruwase, J. Rasley, S. Smith, and Y. He, “Zero-infinity: Breaking the gpu memory wall for extreme scale deep learning,” in *Proceedings of the International Conference for High Performance Computing, Networking, Storage and Analysis*, 2021, pp. 1–14.
- [40] D. Tiwari, S. Gupta, G. Gallardo, J. Rogers, and D. Maxwell, “Reliability lessons learned from gpu experience with the titan supercomputer at oak ridge leadership computing facility,” in *Proceedings of the International Conference for High Performance Computing, Networking, Storage and Analysis*, 2015, pp. 1–12.
- [41] G. Ali, S. Bhalachandra, N. Wright, A. Sill, and Y. Chen, “Evaluation of power controls and counters on general-purpose graphics processing units (gpus).”
- [42] W. Chen, P. Wang, and J. Cheng, “Towards mixed-precision quantization of neural networks via constrained optimization,” in *Proceedings of the IEEE/CVF International Conference on Computer Vision*, 2021, pp. 5350–5359.
- [43] S. Han, H. Mao, and W. J. Dally, “Deep compression: Compressing deep neural networks with pruning, trained quantization and Huffman coding,” in *International Conference on Learning Representations (ICLR)*, 2016.
- [44] M. Zhu and S. Gupta, “To prune, or not to prune: exploring the efficacy of pruning for model compression,” *CoRR*, vol. abs/1710.01878, 2017.
- [45] J. Frankle, G. K. Dziugaite, D. Roy, and M. Carbin, “Pruning neural networks at initialization: Why are we missing the mark?” in *International Conference on Learning Representations*, 2020.
- [46] B. Wu, Y. Wang, P. Zhang, Y. Tian, P. Vajda, and K. Keutzer, “Mixed precision quantization of convnets via differentiable neural architecture search,” *arXiv:1812.00090*, 2018.
- [47] D. Kalamkar, D. Mudigere, N. Mellempudi, D. Das, K. Banerjee, S. Avancha, D. T. Vooturi, N. Jammalamadaka, J. Huang, H. Yuen, J. Yang, J. Park, A. Heinecke, E. Georganas, S. Srinivasan, A. Kundu, M. Smelyanskiy, B. Kaul, and P. Dubey, “A study of BFLOAT16 for deep learning training,” *arXiv:1905.12322*, 2019.
- [48] E. J. Hu, yelong shen, P. Wallis, Z. Allen-Zhu, Y. Li, S. Wang, L. Wang, and W. Chen, “LoRA: Low-rank adaptation of large language models,” in *International Conference on Learning Representations*, 2022.
- [49] P. Stock, A. Joulin, R. Gribonval, B. Graham, and H. Jégou, “And the bit goes down: Revisiting the quantization of neural networks,” in *International Conference on Learning Representations*, 2019.
- [50] C. Zhu, S. Han, H. Mao, and W. J. Dally, “Trained ternary quantization,” in *International Conference on Learning Representations (ICLR)*, 2017.
- [51] S. J. Kwon, D. Lee, B. Kim, P. Kapoor, B. Park, and G.-Y. Wei, “Structured compression by weight encryption for unstructured pruning and quantization,” in *Proceedings of the IEEE/CVF Conference on Computer Vision and Pattern Recognition*, 2020, pp. 1909–1918.
- [52] N. Lee, T. Ajanthan, and P. H. Torr, “Snip: Single-shot network pruning based on connection sensitivity,” in *ICLR*, 2019.